Journal of Engineering, Science and Technological Trends (JESTT)

Vol. 3, Issue 2, July 2026
DOI: https://doi.org/10.64060/JESTT3i21

Article

# Stimuli-Response in Organic Cocrystals with Different Donor-Acceptors

Darya Khan Hassand[1]*, Nawrooz Ali Zahedi[1], Abdul Samad Hamid[1] and Mohammad Sharif Stanikzai[2]

[1]School of Education, Department of Chemistry, Ghazni University, Ghazni 2301, Afghanistan
[2] School of Chemical Industrial Engineering, Department of Petrochemical and Gas Industrial Engineering, Kabul Polytechnic University, Kabul 100, Afghanistan
* Corresponding Email: dk.hassand@gmail.com (D. K. Hassand)

Received: 26 January 2026 / Revised: 23 February 2026 / Accepted: 15 March 2026 / Published online: 11 May 2026



## ABSTRACT

Organic cocrystal engineering refers to the stoichiometric combination of two or more organic molecules through non-covalent intermolecular interactions, but achieving excellent electrical and optical properties remains a challenge due to the lack of clear directions for the rational design of co-crystals. In addition, herein we compare and report these three new cocrystals' chemical and physical properties, crystalline structures and determined response to acid stimuli. This investigation of organic cocrystals contains intermolecular interactions and growth methods, especially the solvent evaporation approach. As a result, we synthesised three new organic cocrystals; among these cocrystals, 3-ATC has the highest response to acid stimuli (different acid fuming). The cocrystal's response time is also in the order of seconds, which is much faster than that of most other stimuli-responsive cocrystals previously described. 3-ATC is a highly sensitive fluorescence switching exhibited under various acid stimuli. But, the other two cocrystals (AETC and DTTC) are strong enough to resist acid stimuli; this is due to the close face-to-face and mixed stacking patterns with CT and π-π interactions. These three cocrystals exhibited different colours and low-dimensional (1D, 2D) morphology structures.

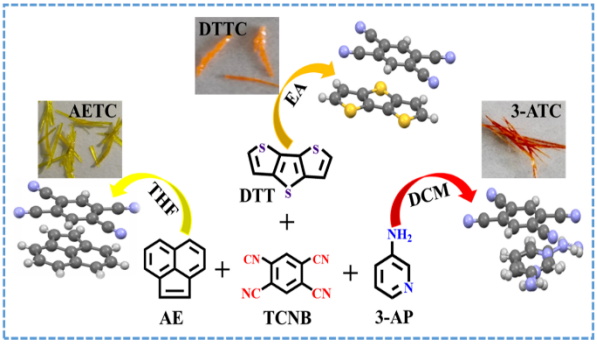


**Keywords:** Acid stimuli; Cocrystal growth; CT interactions; Organic cocrystals; Solvent evaporation

## 1. Introduction

In recent years, there has been an increasing demand for multifunctional materials. Cocrystal engineering is a method that prepares new materials with unique optical and electrical properties using non-covalent bond interactions. This method has gained significant attention [1],[2]. Cocrystallized organic molecules with alkali, alkaline earth salt, inorganic acid, and halogen include haloquinone. The majority of organic cocrystals contain aromatic compounds, including dinitro or Trinitro. It is interesting to note that many cocrystals were discovered by different advanced screening techniques in the 1900 century; some of these have been discovered by scientists in interesting ways [3]. Organic cocrystals have a wide range of applications, including organic field effect transistors (OFETs) [4], photoresponse [5], organic light-emitting transistors (OLETs) [6], room temperature phosphorescence [7], two-photon absorption properties [8] and so on. However, selecting suitable molecules to prepare cocrystals with novel properties is still a great challenge [9]. The organic crystal research field is currently focusing on figuring out how to customise CT and predict the function of cocrystals. Previous studies have mainly focused on selecting the appropriate building blocks to alter the static characteristics of cocrystal formations [10]. Among these, cocrystals made up of easy-to-withdraw acceptors and powerful electron-donating donors are frequently shown to have CT interactions. It is possible to control their activity by mixing various donor and acceptor molecules [11]. At present, the solution approach is the most widely used technique for the

preparation of organic cocrystals [12],[13]. the physical vapour transport (PVT) method [14] and mechanochemical preparation [15]. Different preparation methods allow the preparation of cocrystals with different morphologies, structures and properties. The dissolution method has the advantages of simple operation, flexible design and low cost [16]. In theory, the molecular units of organic cocrystals can be assembled in any molar ratio, but in the existing cocrystal system, the most common are two constituent units and the molecular molar ratio is 1:1 [17]. Designing organic cocrystals with appropriate physical and chemical properties requires an understanding of intermolecular interactions and their influence on crystal stacking. The interactions between different molecules in cocrystals have a non-negligible effect on the properties of cocrystals. Supramolecular interactions in organic cocrystals include charge transfer interactions, π-π interactions, hydrogen bonds, and halogen bond interactions [18]. However, a variety of preparation techniques enable the production of cocrystals with varying morphologies, topologies, and characteristics [19]. The stimulus-responsive behaviours of single-component molecules have been widely studied. However, the investigation of multiple components is still in its primary stages due to the unclear mechanism of cocrystallisation and the uncontrollable functions of the final products. Scientists discovered that the crystal-to-crystal transition between two polymorphs can offer a natural illustration of how to understand the process under the stimuli-responsive mechanism. A timely and insightful study of organic cocrystals toward functional materials is presented, which is expected to open up a new design principle of functional materials for practical applications [20],[21]. In addition, external stimuli can alter intermolecular interactions and even stacking structures, and the degree of CT interaction in cocrystals can be verified and adjusted through experimental methods [22]. A molecular-level structure performance relationship can be established based on organic CT cocrystals to reveal the response mechanism and guide smart cocrystal development.

Herein, we designed and prepared three new organic cocrystals, wherein the TCNB as electron acceptors (A), and three different (AE, DTT and 3-AP) electron donors (D), these cocrystals displays a mixed-stacking arrangement with strong intermolecular interactions, which contributes to the CT nature over the whole supramolecular architecture. Meanwhile, among these cocrystals, the 3-AP molecule in 3-ATC cocrystal can easily interact with the proton because of the weak alkaline nature of their 3-Amide and pyridyl groups, while the degree of CT interactions in 3-ATC can be adjusted by adding electron-withdrawing electropositive hydrogenations. As a result, 3-ATC may respond to various acidic environments and stimuli to change its emission characteristics dynamically (emission colour from red to cream-white; photoluminescence quantum yield from high to low). But the other two cocrystals, AETC and DTTC, were stable against acid stimuli. Therefore, by carefully designing each component, we show how to create an adjustable luminous switching cocrystal system that can be dynamically regulated in response to various acid stimuli. This illustrates the ideal method for creating next-generation smart and multiple functional materials [23]. In addition, those cocrystals in a TCNB-based CT complex system are nearly planar, and stacked alternately on each other, which prompted us to investigate whether the co-assembly of CT complexes with similar acceptor and different donors' structures would emit in yellow, orange and red colours [11].

## 2. Material and Method

### 2.1. Materials

AE (C12H10, 98%), DTT (C8H4S3, 98%), 3-AP (C5H6N2, 99%), and TCNB (C10H2N4, 98%) were the pure single materials, purchased from Shanghai Energy Chemical Corporation, Ltd and Tianjin Xiensi Opod Technology Co., Ltd respectively. Dichloromethane (CH2Cl2), tetra-hydrofuran (THF) and ethyl acetate (EA) were purchased from Tianjin Yuanli Chemical Co., Ltd. Formic acid, Acetic acid, and Hydrochloric acid (HCOOH, CH3COOH, and HCl) solutions were purchased from Tianjin Comeo Chemical Reagent Co., Ltd. and Tianjin Yuanli Chemical Co., Ltd., respectively.

### 2.2. Crystal Growth and Characterisation

The crystal growth process is provided in the supplementary file. After designing and preparing the cocrystals, we investigated and determined their physicochemical properties, performed structural analysis, and carried out further characterisation. Powder X-ray diffraction (PXRD) measurements were conducted using a Rigaku SmartLab diffractometer. Testing parameters: Cu Ka radiation, λ = 1.5418 Å, the power was set to 9 kW, the voltage was 45 kV, and the current was 200 mA. The single-component molecules (AE, DTT, 3-AP, and TCNB) with 5-45 degrees, and the angle interval was 0.01, so PXRD's spectra showed that the organic cocrystals have good quality. The sharp peaks of the cocrystals in PXRD revealed the high quality of the single crystals and the presence of AETC, DTTC, and 3-ATC organic cocrystals, demonstrating that these co-assembled into cocrystals completely during the PVT process.

To determine the structure of the cocrystals, single crystals suitable for X-ray diffraction were chosen, mounted in inert oil in the cold gas stream, and their X-ray diffraction intensity data were collected. On a Rigaku XtaLAB FRX diffractometer equipped with a Hypix6000HE detector, using Cu Kα radiation (λ = 1.54184 Å). Crystal was kept at the temperature listed in the X-ray crystallography section during data collection. The structure was solved by the intrinsic phasing method using SHELXT and then refined with SHELXL in Olex2. Selected details of the data collection and structural refinement can be found within the X-ray crystallography section and full details are available in the corresponding CIF files.

Moreover, crystalline silicon wafers were utilised as the substrate in an optical microscope (OM). Silicon wafers' high atomic-plane structure and clarity made them ideal materials for photographing tiny particles. They are available in several shapes and sizes, and we used the Si-III silicon wafers with sizes of 5 mm × 7 mm and dissolved the same ratio 1:1 molar parent material, i.e., donors and acceptor, in DCM, THF, and EA. The D-A mixture was prepared, and two drops of the solution were applied to a silicon wafer. The OM was utilised to observe and analyse the resulting cocrystal's morphology.

The solid-state samples of the AETC, DTTC, and 3-ATC cocrystals were used for the investigations and determination of photophysical and chemical properties. We used a variety of instrument measurements, including UV-vis, photoluminescence (PL), thermal gravimetric analysis (TGA), differential scanning calorimetry (DSC), and Fourier-transform infrared (FTIR).

The UV-3600 Plus (SHZMADZU, Japan) spectrophotometer, combined with a diffuse reflectance mode integrating sphere, was used for testing the UV-visible diffuse reflectance spectrum. The small amount of powder under the test was evenly applied to the Barium sulfate ($BaSO_4$) substrate. A baseline test of the blank $BaSO_4$ was required to eliminate substrate effects before testing the sample. Cocrystal's powder was directly put on the $BaSO_4$ substrate, thus presenting an absorption spectrum of 300-800 nm and a slit width of 20 nm, which was different compared with the single components and these three Cocrystals.

To further study the PL properties of cocrystals, the emission spectra were obtained on an FL-7000 fluorescence spectrophotometer, and fluorescence micrographs were obtained using a Leica DM2700M optical microscope (300-650 nm) with a plug-in fluorescence unit.

These three solid-state cocrystals were subjected to TGA utilising the TG 209 F3 Tarsus instrument, which is made in Germany by NETZSCH. Under nitrogen gas with cocrystal release dt1.0 and 30-800 °C K/r synchronisation, the TGA was performed. The temperature was set at 10 °C / minute. We also used the DSC technique to observe the melting points of the cocrystals. For this, we used the Polyma instrument manufactured by NETZSCH in Germany and identified single sharp peaks due to melting. The FTIR spectra were obtained using a Bruker Vertex 70 FTIR spectrometer to provide further characterisation. Then, the solid-state cocrystals samples were analyzed using FTIR equipment while nitrogen gas was present. Data were captured by the device between 600 $cm^{-1}$ to 4000 $cm^{-1}$.

## 3. Results and Discussions

### 3.1. Cocrystal Preparation and Its Structure Analysis

Three new organic cocrystals—AETC (CCDC: 2287450), DTTC (CCDC: 2287435), and 3-ATC (CCDC: 2347457)—exhibiting distinct colour emissions and acid-responsive behaviour were designed and prepared. Acenaphthylene (AE), dithieno [3,2-b:2′,3′-d] thiophene (DTT), and 3-aminopyridine (3-AP) were used as electron donors, while tetracyanobenzene (TCNB) served as the electron acceptor. These cocrystals were obtained by slow evaporation of different solutions at room temperature while maintaining the same donor-to-acceptor (D/A) molar ratio. AETC emitted a yellow colour, DTTC an orange colour, and 3-ATC a red colour, different from the colours of their constituents, in that order. According to Figure 1. An extensively performed characterisation technique is X-ray diffraction (XRD), which gives information regarding the crystalline nature and lattice parameters of the material. The PXRD patterns in Figure 2a and S1a display that cocrystals have different peaks from the co-former, indicating successful cocrystallisation instead of the simple sample mixing between different compounds. The measured PXRD result of those cocrystals was consistent with the data calculated through the CIF file.

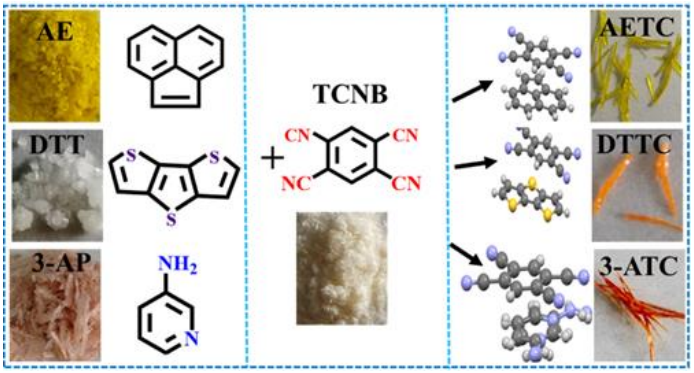


**Figure 1:** *The images and crystal with the molecular structures of AETC, DTTC, 3-ATC, TCNB, 3-AP and AE powder.*

The superstructures of the cocrystals were determined by single-crystal X-ray diffraction analysis. Among the three cocrystals, AETC and DTTC crystallise in the triclinic system, whereas 3-ATC crystallises in the monoclinic crystal system. However, all structures are assigned to the space groups P-1 and C2/c and exhibit a gradual expansion of their lattice parameters: AETC a = 6.73 Å, b = 8.05 Å, c = 15.24 Å, α = 94.33°, β = 99.82°, γ = 97.76 °; DTTC a = 7.22 Å, b = 9.13 Å, c = 12.66 Å, α = 88.45°, β = 94.84°, γ = 95.12°; and 3-ATC a = 7. 24 Å, b = 15.47 Å, c = 11.65 Å, α = 90°, β = 92.67°, γ= 90°. Additional information is provided in Table S1. As seen in Figure 2b-d, the cocrystals' donor and acceptor molecules are stacked face-to-face, displaying a mixed stacking structure. Furthermore, these three cocrystals exhibit short intermolecular donor–acceptor (D–A) contacts, with distances of 3.35 Å for AETC, 3.47 Å for DTTC, and 3.35 Å for 3-ATC. These short contacts suggest that the cocrystals may possess charge-transfer (CT) character. Additionally, the π–π stacking distances between adjacent molecules in the cocrystals are noteworthy. Thus, as can be seen in Fig. S1b-d, for the AETC cocrystal, the N···H–C distances between adjacent donor–acceptor (D–A) molecules within the column are 3.22 and 3.42 Å, while the acceptor–acceptor (A–A) separation is 5.86 Å. Similarly, in the DTTC cocrystal, the N···H–C distances between neighbouring columnar D–A molecules are 2.56 and 3.34 Å, and the A–A distance is 4.33 Å. For the 3-ATC cocrystal, the corresponding N···H–C distances are 3.12 and 3.21 Å, with an A–A separation of 3.33 Å. These intermolecular interactions contribute to the stabilisation of the three cocrystal structures. Depending on the supramolecular interactions operating along the D–A stacking direction and the C–H···N direction, the cocrystals form one- or two-dimensional low-dimensional organic architectures.

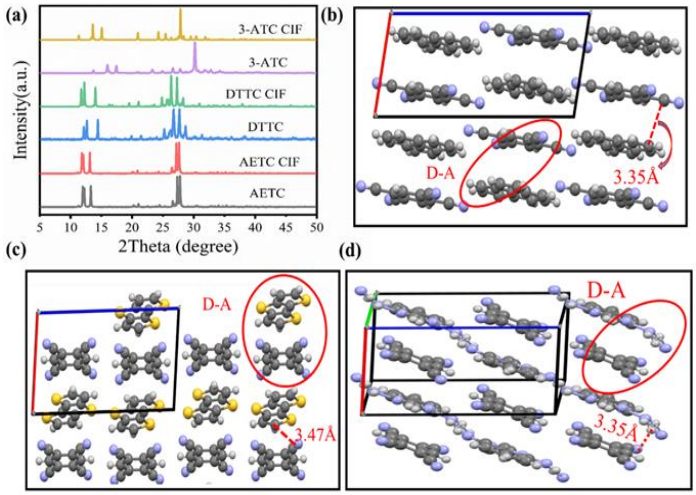


**Figure 2:** *(a) PXRD, (b, c, d) Crystal structures of AETC, DTTC, 3-ATC.*

Moreover, morphological analysis was conducted using optical microscopy (OM) techniques, which suggested a 1D structure for DTTC, 3-ATC cocrystals, and a 2D structure for AETC cocrystals. The OM results explain the centre and edge images of the silicon wafer slide or sample containing these cocrystals, demonstrating their excellent morphology and quality, as shown in Figure S2a-c. Conversely, the D-As are responsible for the donor-acceptor π-π interaction in the AETC, DTTC, and 3-ATC co-crystals as well as the C−H···N strong hydrogen bonds. These three co-crystals' low-dimensional (1D, 2D) morphology results from the comparison of the C−H···N hydrogen bonds to the donor-acceptor π-π interactions along the mixed donor-acceptor stacking direction.

The molecular orbital energy levels of the AETC, DTTC, and 3-ATC cocrystals were calculated using density functional theory (DFT). The results show that the electron density in the HOMO of all three cocrystals is primarily localised on the donor molecules (AE, DTT, and 3-AP). The HOMO energy levels of AETC, DTTC,

and 3-ATC are −6.66 eV, −6.38 eV, and −6.80 eV, respectively, which are close to those of the corresponding pristine donor molecules (−6.05 eV, −5.89 eV, and −6.01 eV). In contrast, the LUMO is mainly distributed over the acceptor molecule (TCNB), with energy levels of −3.678 eV, −3.67 eV, and −4.67 eV for AETC, DTTC, and 3-ATC, respectively, which are comparable to the LUMO energy level of pristine TCNB (−4.06 eV) (Figure 3a and Figure S3). Based on the molecular orbital distributions, the calculated band gaps of DTTC, AETC, and 3-ATC are 2.98 eV, 2.71 eV, and 2.13 eV, respectively. These values are significantly narrower than those of the individual components. Notably, 3-ATC exhibits the smallest band gap among the three cocrystals (Figure S4). The theoretical simulations indicate that the band gap narrowing originates from the charge-transfer (CT) transition between the donor and acceptor molecules. This result is consistent with the observed absorption behaviour, where the cocrystals display different colours (yellow, orange, and red-shifted), corresponding to their progressively reduced band gaps.

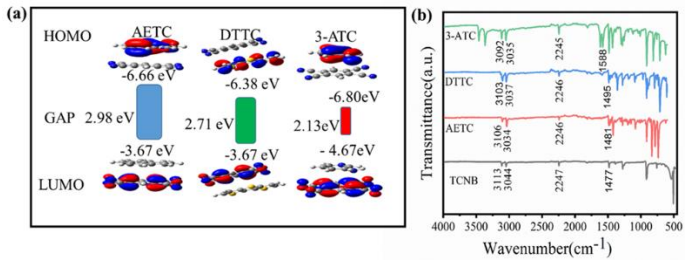


**Figure 3:** *(a) HOMO and LUMO gap, (b) FTIR of AETC, DTTC, and 3-ATC cocrystals.*

Furthermore, Fourier transform infrared spectra (FTIR) spectroscopy was utilised to expose the minute changes in the molecular environment, to gain a deeper understanding of the charge transfer interactions in these three cocrystals. As Fig. 3b illustrates, when compared to the donors, the crystal's broad absorption spectrum, 600 $cm^{-1}$-4000 $cm^{-1}$ is remarkable, and the acceptor demonstrated a robust charge transfer connection with the donors. Additionally, the infrared vibration peaks of the cocrystal almost overlap with those of the pristine components, which demonstrates the successful coassembly. The C–H bond stretching vibration peaks of the acceptor TCNB in the cocrystals red-shift and the C≡N bond stretching vibration peak blue-shifts; the sharp peaks of cocrystals suggest that these three cocrystals have excellent crystal quality. The shift of the cocrystals' peak can be attributed to the various interactions between molecules in the cocrystals. For example, in AETC the TCNB 3113 $cm^{-1}$ band (C–H) is shifted to 3106 $cm^{-1}$,3044 $cm^{-1}$ (C–H) is shifted to 3034 $cm^{-1}$, 2247 $cm^{-1}$(C≡N) is shifted to 2246 $cm^{-1}$, in DTTC the TCNB 3113 $cm^{-1}$ band (C─H) is shifted to 3103 $cm^{-1}$,3044 $cm^{-1}$ (C–H) is shifted to 3037 $cm^{-1}$, 2247 $cm^{-1}$(C≡N) is shifted to 2246 $cm^{-1}$, and in 3-ATC the TCNB 3113 $cm^{-1}$ band (C–H) is shifted to 3092 $cm^{-1}$,3044 $cm^{-1}$ (C–H) is shifted to 3035 $cm^{-1}$, 2247 $cm^{-1}$(C≡N) is shifted to 2245 $cm^{-1}$, the peaks observed in this analysis exhibit varying levels of redshift, indicating a rise in electron cloud density on the benzene ring of the TCNB molecule. These electrons between the D and A molecules reveal the CT characteristic in the cocrystals.

### 3.2. Optical Properties

To get a comprehensive knowledge of the correlation between molecular interactions and photophysical characteristics, we perform in-depth spectroscopic investigations of solid-state crystalline materials. For a complete understanding, various spectra were recorded. Obviously, absorption spectra can be used to distinguish intermolecular interactions. However, the self-assembled three cocrystals show different absorption spectra in the ultraviolet and visible regions with yellow, orange and red shifts of 400 nm, 450 nm and 550 nm, respectively, Figure 4a. These different shifts of the cocrystals in the visible region are due to intermolecular CT from donor to acceptor. Furthermore, DFT calculations of the donor and acceptor molecules indicate that the intermolecular interactions in the cocrystals allow electron delocalisation between the D and A molecules, revealing the CT characteristic in the cocrystals. To further investigate the photoluminescence (PL) properties of the cocrystals, we have measured their PL spectra. The prompt PL spectra exhibit fluorescence emission peaks of AETC, DTTC and 3-ATC located at 500nm, 550nm and 650nm, which exhibit yellow, orange and red colours. As shown in Figure 4b, all these were in the room temperature phosphorescence (RTP) emission and in the solid state of the cocrystals. And different shifts compared to their parents, indicating a small energy gap in the mix-aggregation of the cocrystals, the absorption and emission spectra of the cocrystals based co-forms. In addition, the 2D morphology of the cocrystals increases the specific surface area compared to the 1D structures, which also favours efficient light absorption, strong charge transfer interaction leading to NIR absorption, which is why these three cocrystals show different colours, which are made from different donors with the same acceptor CT and π-π interactions.

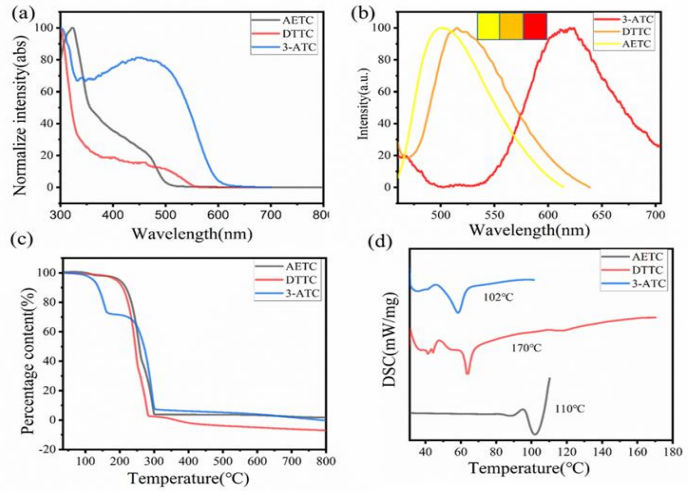


**Figure 4:** *(a) The absorption, (b) fluorescence, (c) TGA, (d) DSC spectra of AETC, DTTTC and 3-ATC in solid-state.*

Thermo-gravimetric analysis and differential scanning calorimetry (TGA-DSC) measurements reveal that the thermal behaviours of these cocrystals are much alike. Having a very similar temperature for every endothermic process (Figure 4c). Their weights are almost constant at 6.9 mg, 8.3mg and 5.07mg, which indicates that the cocrystals are highly stable under the ambient atmosphere and ensure their practical application. Therefore, the stacking mode and relative orientation of the three cocrystals alternated obviously, which would further influence their RTP emission. Those cocrystals (AETC, DTTC and 3-ATC) have decomposition temperatures of 290℃, 280℃, and 200℃. In general, the sublimation temperature of the single component in cocrystals is higher than that of their single crystals, which indicates that the interactions between molecules in the cocrystals are stronger than those in a single-component crystal. The DSC diagram demonstrates that the melting points of those cocrystals are good, which DSC clear diagram shown in Figure 4d. The melting points of these three AETC, DTTC and 3-ATC cocrystals are 110 ℃, 170 ℃ and 102 ℃, respectively, meaning the cocrystals have a

new crystal lattice, and the high melting point indicates that these cocrystals have a stable structure.

## 4. Comparing Cocrystals Protonated through Acidic Stimulation

Binary molecular stacking structures in organic CT complexes can be classified as either mixed or separated stacks. Most in-depth investigations so far have been focused on the former cases due to their unconventional metallic (super) conductivities [24]. Recently, mixed-stack donor–acceptor (D–A) charge-transfer (CT) complexes have been reexamined both theoretically and experimentally because of their promising ferroelectric properties [25]. The offsets of D and A frontier molecular orbitals (FMOs) and their unique molecular arrangement primarily determine the electronic characteristics of the CT structures. Therefore, to develop an effective CT cocrystal system, careful selection of the D/A pair with appropriate FMOs is required.

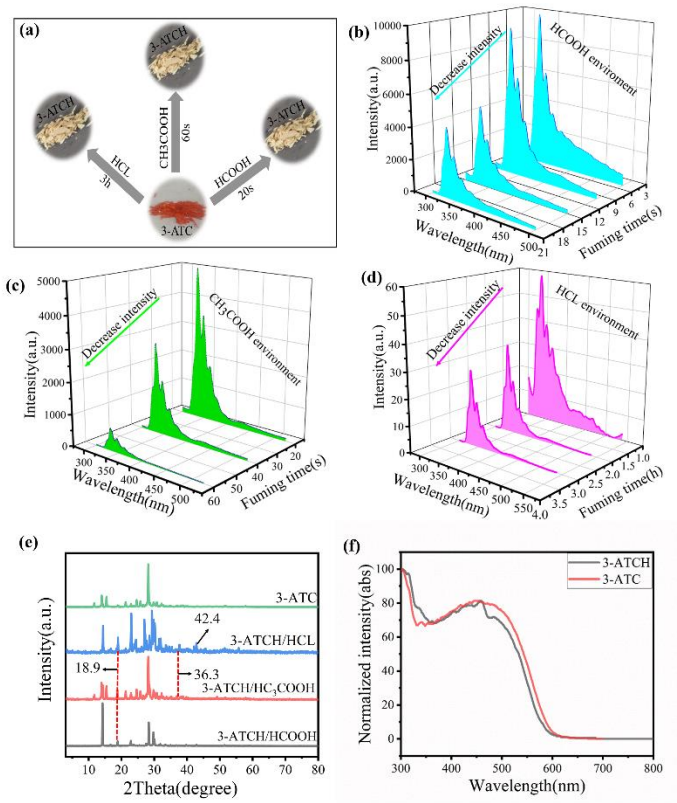


**Figure 5:** *(a) Images of 3-ATC and 3-ATCH, (b-d) decreased intensities of fluorescence of 3-ATCH, (e) PXRD of 3-ATC and 3-ATCH and (f) UV-vis absorption spectra of 3-ATC and 3-ATCH.*

Anyhow, the AE, a polycyclic aromatic hydrocarbon, is an ortho and peri-fused tricyclic hydrocarbon. The molecule resembles naphthalene with positions 1 and 8 connected by a -CH=CH- unit. It is a yellow solid. And the DTT is a conductive material that acts as a donor building block for synthesising a variety of optoelectronic materials. Additionally, the 3-AP, a weak alkaline compound with a 3-amide group and an N atom on the pyridine ring, can readily form pyridinium salts by interacting with protons. However, we employed three different donor molecules with a common acceptor (TCNB) to design organic cocrystals exhibiting acid-stimulated behaviour. The AE- and DTT-based cocrystals are highly stable under various acid stimuli, likely due to the intrinsic structural characteristics of AE and DTT. In contrast, the 3-AP-based cocrystal shows significantly higher responsiveness to acid stimuli. This study shows that the monomer of the 3-AP-based cocrystal changes colour from red to cream-white when it is protonated through acidic stimulation. Thus, the stimuli-responsive luminescent behaviours of the solid-state 3-ATC were explored during protonation. As shown in Figure 5a, the fluorescence colour of the treated 3-ATC samples (called 3-ATCH) changes from red to cream-white, and the luminescence intensity gradually decreases with time and varies in sensitivity with different acids (Figure S5a-c). During the experiment, the samples were exposed to HCOOH, $CH_3COOH$, and HCl vapour for different durations ranging from 5 s to 20 s, 60 s, and 3h. The sensitivity of 3-ATC to formic acid was the highest, with a shorter colour change time of 5 seconds. After exposure to alkaline ($NH_3$) vapour, the fumed ATCH reversibly restores its red emission (Figure S6). The responsive time of 3-ATC is faster than that of most previously reported cocrystals, as shown in Figure 5b-d. To understand this phenomenon, the PXRD patterns of 3-ATC and 3-ATCH were also examined. The PXRD pattern of 3-ATCH shows clear and strong peaks at 18.9°, 36.3° and 42.4°, in contrast to some of the peaks seen in 3-ATC (Figure 5e). It has been shown that the addition of acids during fuming changes the crystal structure of 3-ATC. The 3-ATCH material is a new and unique material with excellent crystallinity. These results suggest that the original 3-ATC and the modified material are combined to form the 3-ATCH sample. CT interactions cause a blue shift in the 3-ATCH absorption region, almost at 500 nm. Due to the electron cloud rearrangement caused by the addition of electron-withdrawing H+ during the smelting process, the band gap of 3-ATCH widens compared to 3-ATC and the D-A interactions become weaker (Figure 5f).

## 5. Conclusion

In summary, the new organic cocrystals of different donors (AE, DTT and 3-Ap) with the same acceptor (TCNB) have been obtained by molecular self-assembly. The complementary electrostatic potential energy of donor and acceptor molecules makes the cocrystals have excellent CT interactions. FTIR spectra, UV–vis absorption spectra, fluorescence spectra, DFT, OM and X-ray diffraction show significant differences in stabilities and photophysical behaviours between cocrystals and single components. As a result, among these cocrystals, 3-ATC exhibits the highest sensitivity to various acid stimuli, with fluorescence switching occurring within seconds. In contrast, the other two cocrystals, AETC and DTTC, are sufficiently robust to resist acid-induced changes. This study provides some suggestions for the preparation of multifunctional organic low- dimensional cocrystals (1D, 2D), and smart materials.

## Declaration

**Acknowledgment:** The authors gratefully acknowledge the financial support from the National Key R&D Program (2022YFA1204401), the Tianjin Natural Science Foundation (20JCJQJC00300), and the Fundamental Research Funds for the Central Universities.

**AI Disclosure:** N/A

**Author Contribution Statement:** D. K. Hassand performed the material preparation and characterisation; N. A. Zahedi, A. S. Hamid and M. Sharif conducted the theoretical calculations; all authors contributed to discussions and manuscript review.

**Availability of Data and Materials**: Data will be made available by the corresponding author on reasonable request.

**Competing Interests:** The authors declare that they have no known competing financial interests or personal relationships that could have appeared to influence the work reported in this paper.

**Consent to Publish:** The authors agree to publish the version of the manuscript in this journal.

**Ethical Issues:** There are no ethical issues.

**Funding Statement:** This work was financially supported by the National Key R&D Program (2022YFA1204401), Tianjin Natural Science Foundation (20JCJQJC00300), and the Fundamental Research Funds for the Central Universities.

## References

1. S. Sato, H. Nikawa, S. Seki, L. Wang, G. Luo, J. Lu, M. Haranaka, T. Tsuchiya, S. Nagase, T. Akasaka, Angew. Chemie - Int. Ed. (2012), 51, 1589–1591.
2. T. Wakahara, P. D'Angelo, K. Miyazawa, Y. Nemoto, O. Ito, N. Tanigaki, D.D.C. Bradley, T.D. Anthop ou los, J. Am. Chem. Soc. (2012), 134, 7204–7206.
3. N. Schultheiss, A. Newman, , Cryst. Growth &Design. (2009), 9, 2950–2967.
4. J. Zhang, H. Geng, T.S. Virk, Y. Zhao, J. Tan, C.A. Di, W. Xu, K. Singh, W. Hu, Z. Shuai, Y. Liu, D. Zhu, Adv. Mater. (2012), 24, 2603–2607.
5. H. Dong, H. Zhu, Q. Meng, X. Gong, W. Hu, Chem. Soc. Rev. (2012), 41, 1754–1808.
6. S.K. Park, J.H. Kim, T. Ohto, R. Yamada, A.O.F. Jones, D.R. Whang, I. Cho, S. Oh, S.H. Hong, J.E. Kwon, J.H. Kim, Y. Olivier, R. Fischer, R. Resel, J. Gierschner, H. Tada, S.Y. Park, Adv. Mater. (2017), 29, 201701346.
7. B. Zhou, Q. Zhao, L. Tang, D. Yan, Chem. Commun. (2020), 56, 7698–7701.
8. L. Sun, W. Zhu, W. Wang, F. Yang, C. Zhang, S. Wang, X. Zhang, R. Li, H. Dong, W. Hu, Angew. Chemie - Int. Ed. (2017), 56, 7831–7835.
9. M. Jiang, S. Li, C. Zhen, L. Wang, F. Li, Y. Zhang, W. Dong, X. Zhang, W. Hu, Front. Optoelectron. (2022), 15, 1–10.
10. J. Jin, S. Wu, Y. Ma, C. Dong, W. Wang, X. Liu, H. Xu, G. Long, M. Zhang, J. Zhang, W. Huang, ACS Appl. Mater. Interfaces. (2020), 12, 19718–19726.
11. Y.L. Lei, Y. Jin, D.Y. Zhou, W. Gu, X.B. Shi, L.S. Liao, S.T. Lee, Adv. Mater. (2012), 24, 5345–5351.
12. D. Khan, M.A.B.A , Zhang Xiaotao, Muhammad Hasnain Jameel, uhammad S.B.R. and M.A. MBajaber, Micro Nano Syst. Lett. (2023), 11:24, 2- 9.
13. S. Li, D. Yan, ACS Appl. Mater. Interfaces. (2018), 10, 22703–22710.
14. H. Jiang, C. Kloc, MRS Bull. (2013), 38, 28–33.
15. D. Braga, L. Maini, F. Grepioni, Chem. Soc. Rev. (2013), 42, 7638–7648.
16. M. Jiang, C. Zhen, S. Li, X. Zhang, W. Hu, Front. Chem. (2021), 9, 1–16.
17. H. wenping zhu weigang, zhen yonggang, Dong huanli, Fu hongbing, Prog. Chem. (2014), 26, 1292–1306.
18. Y.L. Lei, L.S. Liao, S.T. Lee, J. Am. Chem. Soc. (2013), 135, 3744–3747.
19. Y. Liu, Q. Zeng, B. Zou, Y. Liu, B. Xu, W. Tian, Angew. Chemie - Int. Ed. (2018), 57, 15670–15674.
20. L. Sun, W. Zhu, F. Yang, B. Li, X. Ren, X. Zhang, W. Hu, Phys. Chem. Chem. Phys. (2018), 20, 6009–6023.
21. L. Sun, Y. Wang, F. Yang, X. Zhang, W. Hu, Adv. Mater. (2019), 31, 1–22.
22. Y. Liu, A. Li, S. Xu, W. Xu, Y. Liu, W. Tian, B. Xu, Angew. Chemie - Int. Ed. (2020), 59, 15098–15103.
23. W. Hu, H. Zhang, K. Salaita, H. Sirringhaus, SmartMat. (2020), 1, 1014.
24. D. Jérome, A. Mazaud, M. Ribault, K. Bechgaard, D. Jérome, A. Mazaud, M. Ribault, K. Bechgaard, HAL. (2008), 23, 1730.
25. Y. Zhai, S. Li, J. Li, S. Liu, T.D. James, J.L. Sessler, Z. Chen, Nat. Commun. (2023), 14, 1–10.

## Author(s) Bio

**Darya Khan Hassand** was born in Paktika province in Afghanistan. Received his BSc in 2009 in the Chemistry and Biology Department at Sheikh Zayed University Khost-Afghanistan. He completed his MSc in 2020 Organic Chemistry from Tianjin University in Tianjin, China and He completed Ph.D at Tianjin University in China. He is working as an associate professor at Ghazni University Ghazni-Afghanistan. His research area includes the synthesis of Organic Semiconductors, organic optoelectronic devices, and Organic Cocrystals functional and smart materials. He will be the author of Advanced Nanomaterials for High-Performance Sensors 2nd Chapter book and a contributor/associate editor in Ghazni University's national journal and also in Muslim university's Ghazni Afghanistan international journal. Along with different high-ranking journal articles; he also participated in various reputed international conferences.
*Email: dk.hassand@gmail.com*

**Nawrooz Ali Zahedi** was born in 1367 in the Borujagi area of Nawar district of Ghazni province. He graduated from the Chemistry Department at the University of Education and Training in Kabul. Then In 1396, he left for the Islamic Republic of Iran using a scholarship from the Ministry of Science of Iran and joined the Faculty of Chemistry, Department of Organic Chemistry, and Tehran University. In addition, he completed his master in 2019. He has 12 years of teaching experience at Ghazni University, Ghazni Province, currently, he is working as an assistant professor at Ghazni University Ghazni-Afghanistan.
*Email: nawroozali.af@gmail.com*

**Abdul Samad Hamid** was born in the Qarbagh district of Ghazni province. He graduated from the Chemistry Department at the Qandahar University of Qandahar Afghanistan. . Then, he left for the Islamic Republic of Iran using a scholarship from the Ministry of Science of Iran and joined the Faculty of Chemistry, Department of Organic Chemistry, and Tehran University. In addition, he completed his master degree, currently, he is working as an assistant professor at Ghazni University Ghazni-Afghanistan.
*Email: abdulsamadhamid39@gmail.com*

**Mohammad Sharif Stanikzai** obtained his bachelor's degree in chemical technology in 2016, and April 2024, He don his master's degree from Kabul Polytechnic University Kabul Afghanistan. He has served in various positions. Finally, due to his special interest in teaching, in 2019 he started work as a lecturer in the faculty of Petrochemical and Gas Industrial Engineering at Kabul Polytechnic University. Now he works as a young educated scientist and Assistant Professor.
*Email: sharif@kpu.edu.af*